

# Acetylene formation during the catalytic oxidative dehydrogenation of ethane over Pt-coated monoliths at short contact times

Derrick W. Flick and Marylin C. Huff\*

*Department of Chemical Engineering, University of Delaware, Newark, DE 19716, USA*  
E-mail: huff@che.udel.edu

Received 18 April 1997; accepted 20 June 1997

Short contact time monolithic reactors have been examined for the production of ethylene by oxidative dehydrogenation over a supported Pt catalyst. The results so far suggest that these reactors may revolutionize the way chemical synthesis is conducted, but many questions remain. This paper addresses the co-production of acetylene. Under some conditions, acetylene is produced as a by-product during the oxidative dehydrogenation of ethane. This acetylene formation appears to be due to homogeneous reactions since the acetylene production increases at higher reaction temperatures and under conditions where there is little available surface area for radical quenching.

**Keywords:** oxidative dehydrogenation, ethylene, acetylene, monoliths, surface-generated free radicals, combustion

## 1. Introduction

Oxidative dehydrogenation of ethane over Pt-coated monolith catalysts at short contact times has been investigated concerning the maximization of  $C_2H_4$  production [1,2]. In the previous work, acetylene production was typically less than the sensitivity of the analysis. Under the conditions of maximum ethylene production, acetylene formation is indeed negligible, as we will show. Previous work further assumed that at the short contact times achieved in the monolithic reactor, the contribution of homogeneous reactions is negligible. However, these autothermal, monolithic reactors often operate at temperatures in excess of  $800^\circ\text{C}$  where the rates of homogeneous reaction are comparable to the rates of heterogeneous reactions.

Although  $C_2H_4$ , CO,  $H_2$ , and  $H_2O$  are the dominant products, we have found that acetylene is also formed during the oxidative dehydrogenation of  $C_2H_6$  over monolith catalysts under some conditions. In this paper, we examine those conditions and suggest routes to the minimization of undesirable by-products. Acetylene production is potentially a good indicator of the contributions of homogeneous reactions. Thermal dehydrogenation, pyrolysis, can proceed through a free-radical Rice–Herzfeld mechanism [3–5]. In the presence of a Pt catalyst, surface OH forms readily [6–14] and can desorb into the gas phase and initiate and propagate the homogeneous reactions [15,16].

## 2. Experimental

The reactor is essentially identical to that previously described for the production of syngas [17] and oxidative dehydrogenation of ethane [1]. The reactor operates very nearly adiabatically. The catalyst is prepared as described previously from a 45 ppi (pores per linear inch) ceramic foam monolith (92%  $\alpha\text{-Al}_2\text{O}_3$ , 8%  $\text{SiO}_2$ ) that is impregnated with a saturated solution of  $H_2PtCl_6$  [1,17]. The catalyst used in this study was 5.88 wt% Pt.

The feed gas consists of  $C_2H_6$  and  $O_2$  with  $N_2$  as the diluent. All flow rates are controlled with Brooks electronic mass flow controllers with the accuracy of  $\pm 0.2$  SLPM for each component. The level of dilution ranged from 20 to 80%. The  $N_2$  was used as an internal GC calibration standard and as a buffer to control the flammability of the reactant mixture. All product concentrations except  $H_2O$  are measured relative to GC calibration standards. The  $H_2O$  in the product is calculated by an oxygen atom balance. The remaining atom balances, carbon and hydrogen, closed to within  $\pm 10\%$ .

Although most data is collected in the presence of sufficient  $N_2$  dilution and at high enough fuel to oxygen ratios that the reactant mixture is not flammable, some experiments have been conducted within the flammability limits of stationary mixtures of  $C_2H_6$ ,  $O_2$ , and  $N_2$  ( $C_2H_6/O_2 = 1.2$ ,  $N_2 = 20\text{--}50\%$ ). These are the cases that lead to the most production of  $C_2H_2$ . While these mixtures are flammable when stationary, the flow rate through the reactor is sufficiently high that the velocity through the premixed portion of the reactor exceeds the homogeneous flame speed thus preventing explosion.

The reaction temperature is measured by a type R (Pt–Pt/13% Rh) thermocouple inserted from the rear of

\* To whom correspondence should be addressed.

the reactor and placed at the center of the reactor tube between the catalyst and the rear radiation heat shield. The temperature at the front of the catalytic monolith is measured by a type K (chromel/alumel) thermocouple that is located between the catalyst and the front heat shield. The temperature measured at the back of the catalytic monolith, the exit temperature, is a fairly good measure of both the gas-phase temperature and the surface temperature of the rear face of the catalyst. At the catalyst exit, the gas-phase and surface temperatures approach equilibrium. Additional (stationary and movable) thermocouples are used to monitor the temperature profile after the catalyst.

### 3. Results

#### 3.1. Ethane in $O_2$ : low nitrogen dilution

In figure 1 we show results for ethane oxidation over a 5.88 wt% Pt/ $\alpha$ - $Al_2O_3$  foam monolith. Figure 1a shows

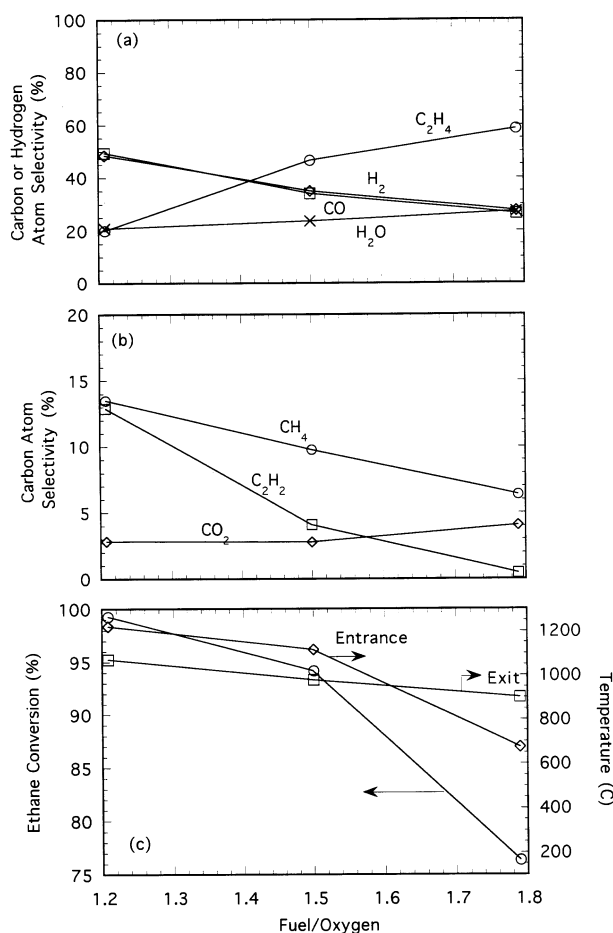


Figure 1. Carbon atom and hydrogen atom selectivity (a, b), ethane conversion (c), and catalyst temperature (c) for ethane oxidation over a 45 ppi, 5.88 wt% Pt/ $\alpha$ - $Al_2O_3$  foam monolith as a function of the  $C_2H_6$  to  $O_2$  ratio in the feed with 20%  $N_2$  dilution with a total feed flow rate of 2 SLPM in an autothermal reactor at a pressure of 1.2 atm.

that the selectivity to  $CO$  and  $H_2$  parallel each other (the  $CO$  selectivity is calculated on a carbon atom basis and the  $H_2$  selectivity is calculated on a hydrogen atom basis) and decrease at higher fuel to oxygen ratios. Likewise, the selectivity to both  $C_2H_4$  and  $H_2O$  increase at higher fuel to oxygen ratios as we approach the stoichiometry for the oxidative dehydrogenation reaction.

Figure 1b shows that the selectivity to acetylene falls with increasing ethane concentration in the feed. The acetylene selectivity steadily decreases from 13% at a fuel to oxygen ratio of 1.2 to less than 1% at a fuel to oxygen ratio of 1.8. This suggests that acetylene formation is more significant at low fuel to oxygen ratios where the adiabatic reaction temperature is highest. Figure 1c shows that the ethane conversion falls from > 99% at 1.2  $C_2H_6/O_2$  to ~ 76% at 1.8  $C_2H_6/O_2$ . The oxygen conversion also falls with increasing ethane composition, but is always greater than 99%. The reaction temperature at the exit of the monolith decreases smoothly with increasing fuel composition from 1030 to 900°C. The temperature at the entrance of the monolith changes drastically with feed composition. At 1.2  $C_2H_6/O_2$ , the reaction temperature at the entrance is 1200°C, nearly 100°C higher than the exit temperature, and falls to 680°C at 1.8  $C_2H_6/O_2$ .

#### 3.2. Ethane in $O_2$ : high nitrogen dilution

High levels of reactant dilution have a tremendous effect on the reaction (rear) temperature in this adiabatic reactor. Changing the level of dilution from 20 to 80%  $N_2$  decreases the catalyst exit temperature by ~ 200°C. The major reaction products, at reduced ethane conversion, under these conditions are water, carbon monoxide, and carbon dioxide with a higher selectivity to  $CO_2$  and corresponding lower selectivity to  $CO$  at higher ethane compositions. At these lower temperatures, acetylene is not observed as a reaction product and only a trace amount of methane is formed.

#### 3.3. Preheat

In figure 2, the effects of preheating the feed are shown. Results are shown as a function of fuel to oxygen ratio for nearly adiabatic operation (without preheat) and for autothermal operation where the reactants have been heated to 300°C before reaching the reaction zone. Preheat leads to a lower selectivity to ethylene and correspondingly higher selectivity to acetylene. The selectivity to hydrogen also increases with preheat while the selectivity to  $H_2O$  decreases. As expected, the ethane conversion increases with preheat. The catalyst temperature decreases slightly with preheat. This is a relic of the temperature measurement procedure. The reported "catalyst temperature" is the catalyst exit temperature. When the reactants are preheated, the oxygen is consumed more quickly resulting in a more pronounced

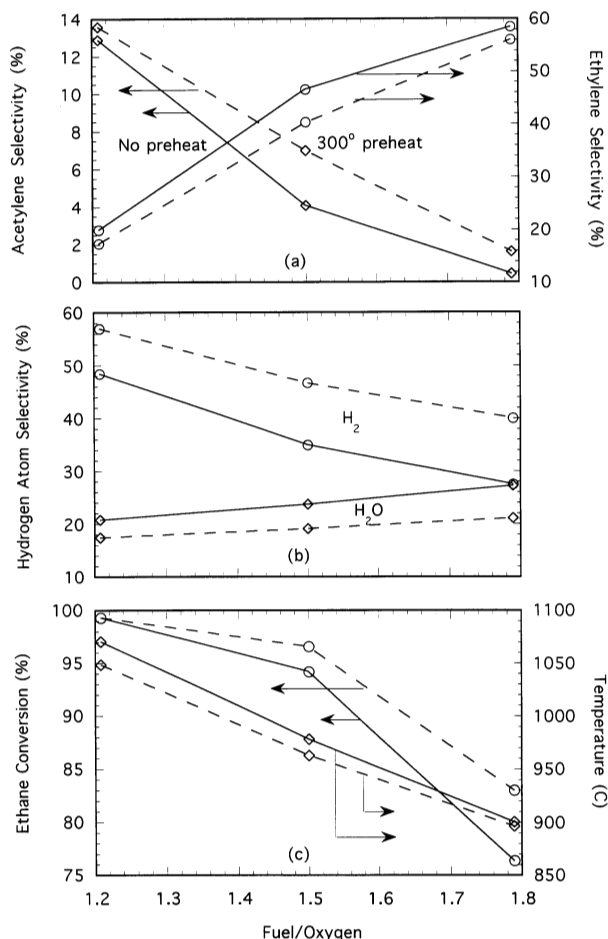


Figure 2. Acetylene and ethylene selectivity (a), hydrogen atom basis selectivity (b), ethane conversion (c), and catalyst exit temperature (c) for ethane oxidation over a 45 ppi, 5.88% Pt/ $\alpha$ - $Al_2O_3$  foam monolith as a function of the  $C_2H_6$  to  $O_2$  ratio in the feed with 20%  $N_2$  dilution with a total feed flow rate of 2 SLPM in an autothermal reactor at a pressure of 1.2 atm. The solid lines represent the reactor with no preheat of the feed (figure 1). The dashed lines represent the reactor with a feed preheat of 300°C.

axial temperature gradient. The front of the catalyst is hotter while the rear is slightly cooler.

### 3.4. Flowrate

The solid lines in the right panels in figure 3 illustrate the effect of increased flow rate (12 SLPM). For comparison, the data in figure 1 (2 SLPM) is shown with the solid lines in the left panels. For now, ignore the dashed lines. While the selectivities to the major products  $C_2H_4$ ,  $H_2O$ , CO, and  $H_2$  are very similar at both flow rates, the fuel to oxygen ratio has a greater effect on acetylene selectivity at the higher flow rate and the ethane conversion increases at the higher flow rate.

## 4. Discussion

To summarize these results, on a Pt-coated monolith up to 15% of the ethane is converted to acetylene at  $\sim 1100^\circ C$  at contact times of  $\sim 10$  ms in a steady-state reactor with nearly complete conversion of  $C_2H_6$  and  $O_2$ . Higher flow rates result in higher ethane conversion without significant changes in the product selectivity. Higher reaction temperatures tend to increase the selectivity to acetylene and hydrogen. In this essentially adiabatic reactor, higher reaction temperatures are obtained by preheating the feed and/or reducing the level of dilution. Both of these routes also lead to increased ethane conversion. Preheat has little effect on the CO and  $CO_2$  selectivity; whereas, high levels of dilution tend to cause higher selectivity to the combustion products,  $CO_2$  and  $H_2O$ .

### 4.1. Reaction mechanism

In previous research [1,18], an oxidative dehydrogenation mechanism was suggested for ethane. This mechanism, as outlined in figure 4, addresses several important factors: (1) the absence of carbon deposition under conditions where it is thermodynamically favorable, (2) the role of oxygen in the heterogeneous reaction, and (3) the increase of ethylene production at higher reaction temperatures. The mechanism, however, does not include the non-selective homogeneous gas-phase reactions that can take place at elevated temperatures. These homogeneous reactions occur in the open reactor tube before and after the catalyst and heat shields and in the gas space within the catalytic monolith and heat shields. The empty reactor tube provides a low amount of surface area to scavenge the free-radical chain propagators necessary for homogeneous reaction and subsequent acetylene production, but the temperature is much greater in the immediate vicinity of the catalyst where significantly more quenching surface area is available. It is quite likely that the OH surface species desorb and propagate gas-phase free-radical reactions at sufficiently high temperatures.

This free-radical chemistry will also lead to gas-phase production of  $C_2H_4$  from  $C_2H_6$ . For the purposes of this discussion, we assume that the homogeneous production of  $C_2H_4$  is negligible compared to the heterogeneous production of  $C_2H_4$  and that the heterogeneous production of  $C_2H_2$  is negligible compared to the homogeneous production of  $C_2H_2$ . Based on experiments made in the absence of Pt catalyst at elevated temperatures and relatively short contact times, it is estimated that homogeneous reactions may account for no more than 20% of the conversion of  $C_2H_6$  [19]. Conversely, the  $C_2H_2$  that is formed on the surface is more apt to contribute to coking or  $CO_x$  formation than desorb. The homogeneous and heterogeneous reactions are coupled, but uncoupling them leads to some interesting conclusions.

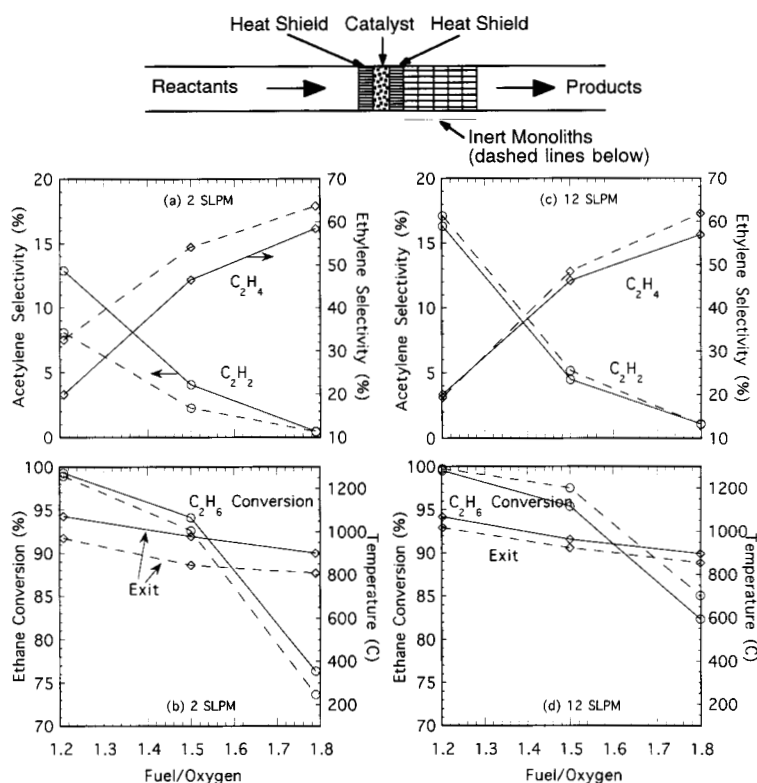


Figure 3. Acetylene and ethylene selectivity (a, c) and ethane conversion and catalyst exit temperature (b, d) for ethane oxidation over a 45 ppi, 5.88% Pt/ $\alpha$ - $\text{Al}_2\text{O}_3$  foam monolith as a function of the  $\text{C}_2\text{H}_6$  to  $\text{O}_2$  ratio in the feed with 20%  $\text{N}_2$  dilution with a total feed flow rate of 2 SLPM (a, b) and 12 SLPM (c, d) in an autothermal reactor at a pressure of 1.2 atm. The plots on the left are for the low flow rate and the plots on the right are for the high flow rate. The dashed lines correspond to data collected under the same conditions, but with inert monoliths placed downstream of the catalyst.

#### 4.2. Axial temperature profile

A typical temperature profile for the monolith reactor at 2 SLPM is shown in figure 5 (solid curve). The reactants enter the reactor at  $25^\circ\text{C}$  and are quickly heated to  $\sim 1000^\circ\text{C}$  at the front of the catalyst. After the product gases leave the catalytic monolith, the temperature falls quickly to  $220^\circ\text{C}$ . In fact, the temperature is  $\sim 800^\circ\text{C}$  at the exit of the heat shield and falls  $200^\circ\text{C}$  to  $\sim 600^\circ\text{C}$  at 1 cm behind the heat shield. In figure 5, we also show the typical temperature profile for the reactor at 12 SLPM (dashed curve). Again, the reactants are quickly heated from 25 to  $\sim 1150^\circ\text{C}$ . However, at the higher flow rates, the rear thermocouple measures a higher gas-phase temperature than the front thermocouple. The front thermocouple is measuring the gas-phase temperature of the reactants just before they enter the hot catalyst before thermal equilibrium has been obtained. After the product gases exit the catalyst, the temperature falls more slowly to around  $880^\circ\text{C}$  at 11 cm behind the catalyst compared to  $200^\circ\text{C}$  for the same location for the slower flow rate.

The slight difference in acetylene selectivity with flow rate shown with the solid curves in figure 3 can be partially explained by comparing the temperature profiles

for the two cases. At 2 SLPM, the products are quickly quenched from  $1000^\circ\text{C}$  to less than  $600^\circ\text{C}$  within a couple of centimeters from the catalyst. This quenching is accomplished by heat loss through the uninsulated reactor walls after the catalyst zone. This quenching retards the production of free radicals necessary for the homogeneous reactions. Therefore, there should be evidence of only minor amounts of homogeneous reaction and acetylene production. At 12 SLPM, the product temperature falls much more slowly from 1000 to  $880^\circ\text{C}$  at a distance 11 cm behind the catalyst. Therefore, the products are at an elevated temperature for a longer period of time. Since the products are not quenched as quickly, there should be more homogeneous reaction and more formation of acetylene.

#### 4.3. Homogeneous reactions

In our experiments, the acetylene is most likely produced by the homogeneous pyrolysis of ethylene in the gas space within the monolith [3–5]. On the Pt surface, OH forms rapidly and at high temperatures, some OH-radicals will desorb and exist in the gas phase [15]. These OH $\cdot$  species can initiate the process for  $\text{C}_2\text{H}_2$  production. The selectivity to acetylene should depend on the

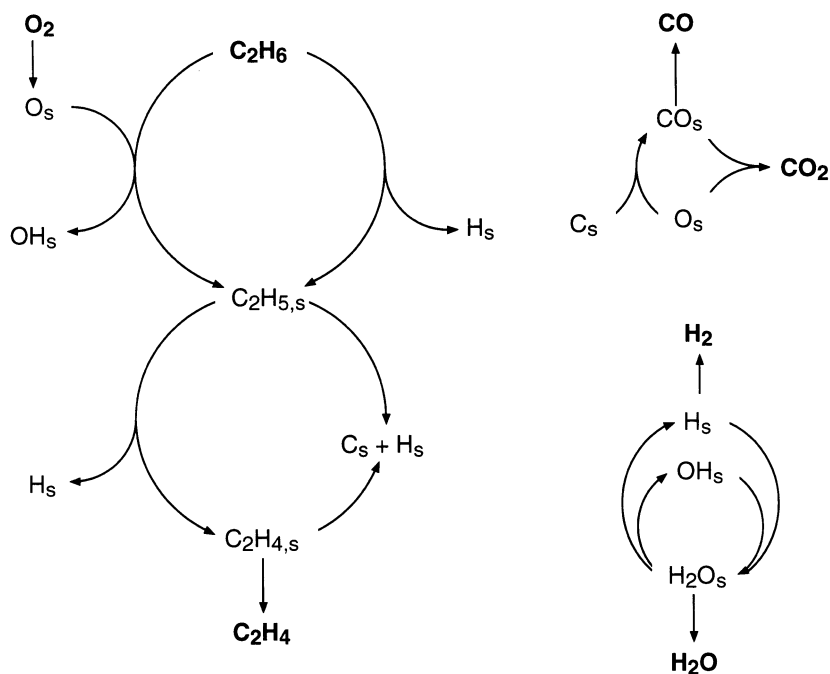


Figure 4. Simplified depiction of the heterogeneous reaction mechanism for ethane oxidation over a Pt catalyst [1,18]. In the interest of simplicity of the diagram, the reactions leading to  $C_2H_4$ , CO and  $CO_2$ , and  $H_2$  and  $H_2O$  have been separated into three distinct sets. The gas-phase species are shown in bold type. All other species are assumed to be adsorbed to the Pt surface.

temperature for generation of radicals and propagation of the homogeneous reactions and on the available surface area for quenching of radicals. To test this surface-area dependence, we filled the section behind the reactor with additional inert monoliths whose solid surfaces scavenge the free-radical propagators necessary for the production of acetylene.

In figure 3, we show the selectivity, conversion, and catalyst temperature for the reactor with (dashed curves)

and without (solid curves) additional monoliths inserted after the catalyst. A schematic of the reactor with additional monoliths is also shown. The plots on the left side and right side are for data collected with a total flow rate of 2 and 12 SLPM, respectively. Although this data is not shown, the addition of inert monoliths behind the catalyst does not significantly affect the temperature profile. The temperature difference between the two configurations did not differ by more than  $10^\circ\text{C}$  at any position.

The additional monoliths, however, did create a larger pressure drop through the reactor. Since the reactor exit pressure was maintained constant at 1.2 atm, this led to a slightly higher pressure at the catalytic monolith when the downstream monoliths were in place. With the addition of extra inert monoliths behind the catalyst, the acetylene selectivity is lower and the ethylene selectivity is higher for all fuel to oxygen ratios for the lower flow rate case. However, the  $C_2H_6$  conversion and temperature at the catalyst's exit were also slightly lower. At the higher flow rate, the difference is much less pronounced.

Computer simulation of this reaction system using the mechanism shown in figure 4 supports the increased ethylene and water selectivity as well as the reduced selectivity to CO and  $H_2$  and the reduced overall ethane conversion. The model, however, does not allow for  $C_2H_2$  production or any homogeneous reaction, so it cannot be used to explain the  $C_2H_2$  selectivity trends. At the temperatures of these experiments, the rates of the termination steps control the amount of homogeneous reaction. At higher pressure, the rate of termination of

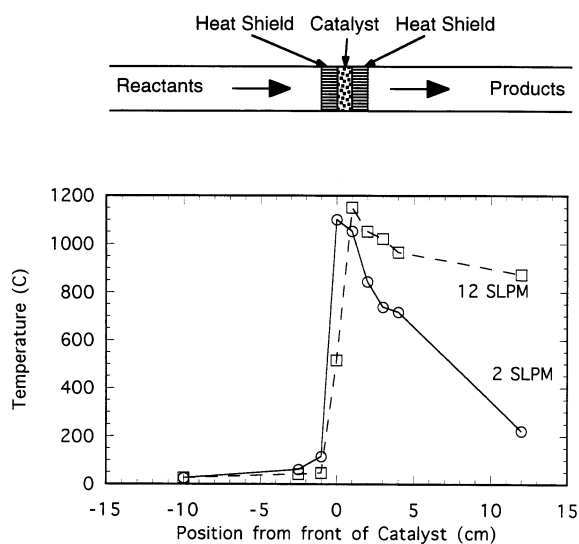


Figure 5. Schematic of the reactor, and the temperature profile for the reactor plotted as a function of the distance from the front of the catalyst at 2 and 12 SLPM at  $C_2H_6/O_2 = 1.2$  and 20%  $N_2$  dilution.

the radicals increases slowing the overall rate of the free-radical reactions and reducing the production of  $C_2H_2$ .

The free-radical mechanism can also explain the difference in acetylene formation at different inert dilutions. Of course, the bulk of the selectivity and conversion variation can be attributed to the reaction temperature in the adiabatic reactor that is a strong function of the level of dilution. In addition, at low inert dilution, the concentration of reacting species is higher, thereby resulting in a higher probability of collision and reaction. At higher dilution, the reactant concentrations are much lower which corresponds to a lower collision frequency and lower selectivity to acetylene.

#### 4.4. Reaction times

The correspondence between the length of time that the temperature exceeds  $800^\circ C$  and acetylene selectivity is shown in figure 6a. The reaction time was calculated by using the temperature profiles shown in figure 5. The times shown in figure 6a are a function of the reactor volume, the monolith void fraction ( $\epsilon = 0.8$ ) [20,21], and the actual volumetric flow rate that is in turn a function of the temperature, pressure, and extent of reaction (mole change).

In cases where the gases spend less than 0.014 s at high temperatures ( $> 800^\circ C$ ), there is negligible acetylene formation. However, when the gases are hot for longer times, acetylene selectivity increases. Thus, the longer the reaction temperature is above  $800^\circ C$ , the higher the acetylene selectivity. The spread of data at longer reaction times is due to (1) the error induced by the interpolation between the measured temperature positions, (2) the rather arbitrary  $800^\circ C$  temperature limit and the fact that the maximum temperature is not considered at all, and (3) errors in the carbon balance from the GC analysis.

#### 4.5. Time-average reaction temperature

Figure 6b addresses dependence of acetylene selectivity on the time-average gas-phase temperature. The temperatures shown in figure 6b were calculated as follows:

$$\bar{T} = \frac{1}{t_2 - t_1} \int_{t_1}^{t_2} T(t) dt, \quad (1)$$

where  $t_1$  and  $t_2$  are measures of residence time corresponding to the positions in the reactor where the temperature first exceeds  $800^\circ C$  and drops below  $800^\circ C$ , respectively. Data is also shown for cases where the temperature never exceeded  $800^\circ C$  and no acetylene was formed. For these cases,  $t_1$  and  $t_2$  correspond to the points at which the gases entered and left the catalyst.

The strong correlation between the average temperature and acetylene selectivity supports the assertion that

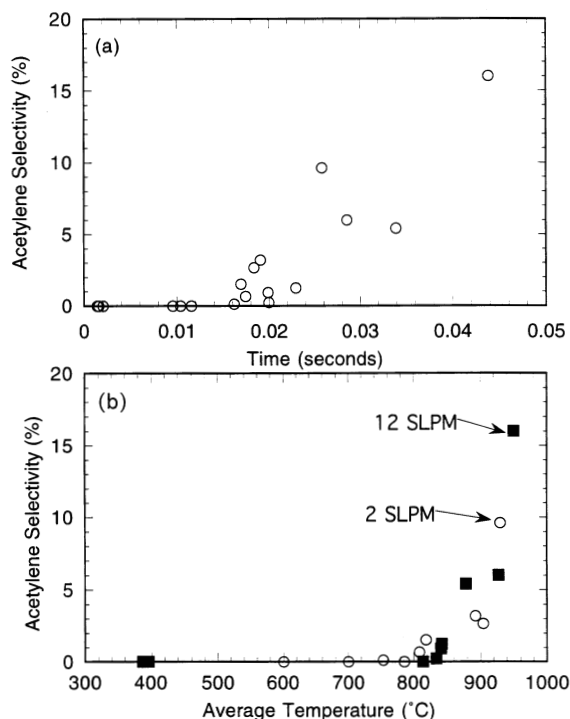


Figure 6. Acetylene selectivity (a) as a function of the time that the temperature is above  $800^\circ C$  and (b) as a function of the time-average temperature in the reaction zone for ethane oxidation over a 45 ppi, 5.88 wt% Pt/ $\alpha$ - $Al_2O_3$  foam monolith. The data shown here is a compilation of data collected at a variety of flow rates, levels of dilution, fuel to oxygen ratios, and levels of preheat.

acetylene formation is due to homogeneous reactions and that the rates of these reactions increase at elevated temperatures. This figure clearly shows that acetylene production becomes significant only when the reaction temperature is very high. This corresponds to reaction conditions with little diluent or at low fuel to oxygen ratios within the flammability limits or near the upper flammability limit.

## 5. Conclusions

We find that acetylene is produced during the oxidative dehydrogenation of ethane in a monolith reactor at short contact times under some reaction conditions. The acetylene formation is due to the non-selective homogeneous reactions that can take place in the open reactor tube before and after the catalyst and in the gas space within the catalytic monolith and heat shields. The acetylene is most likely formed by gas-phase reactions initiated by surface-generated radicals. By increasing the surface area for radical quenching, acetylene selectivity decreases with a corresponding increase in ethylene selectivity. The acetylene selectivity is also shown to be dependent on the time that the gas is above  $800^\circ C$  and the degree to which the temperature exceeds  $800^\circ C$ . At very short times where the gas is above  $800^\circ C$ , there is

negligible acetylene formation. While at longer times and/or at higher temperature, acetylene selectivity increases.

## References

- [1] M. Huff and L.D. Schmidt, *J. Phys. Chem.* 97 (1993) 11815.
- [2] P.M. Witt and L.D. Schmidt, *J. Catal.* 163 (1996) 465.
- [3] Z. Renjun, *Fundamentals of Pyrolysis in Petrochemistry and Technology* (Citic, Beijing, 1993).
- [4] L.F. Albright, B.L. Crynes and W.H. Corcoran, *Pyrolysis: Theory and Industrial Practice* (Academic Press, New York, 1983).
- [5] J.W. Moore and R.G. Pearson, *Kinetics and Mechanism* (Wiley, New York, 1981).
- [6] C.M. Marks and L.D. Schmidt, *Chem. Phys. Lett.* 178 (1992) 358.
- [7] S. Ljungstrom, B. Kasemo, A. Rosen and T. Wahnstrom, *Surf. Sci.* 216 (1989) 63.
- [8] D.S.Y. Hsu and M.C. Lin, *Appl. Surf. Sci.* 28 (1987) 415.
- [9] G.S. Selwyn, G.T. Fujimoto and M.C. Lin, *J. Phys. Chem.* 86 (1982) 760.
- [10] C.E. Mooney, L.C. Anderson and J.H. Lunsford, *J. Phys. Chem.* 95 (1991) 6070.
- [11] T.A. Griffin, L.D. Pfefferle, J.J. Dyer and D.R. Crosley, *Combustion Sci. Technol.* 65 (1989) 19.
- [12] N.J. Brown, R.W. Schefer and F. Robben, *Combustion Flame* 51 (1983) 263.
- [13] V.J. Kwasniewski and D.J. Schmidt, *J. Phys. Chem.* 96 (1992) 5931.
- [14] W.R. Williams, C.M. Marks and L.D. Schmidt, *J. Phys. Chem.* 96 (1992) 5922.
- [15] J.H. Lunsford, E. Morales, D. Dissanayake and C. Shi, *Int. J. Chem. Kinet.* 26 (1994) 921.
- [16] K.T. Nguyen and H.H. Kung, *Ind. Eng. Chem. Res.* 30 (1991) 351.
- [17] D.A. Hickman and L.D. Schmidt, *J. Catal.* 138 (1992) 267.
- [18] M.C. Huff and L.D. Schmidt, *AIChE J.* 42 (1996) 3484.
- [19] D.A. Goetsch and L.D. Schmidt, *Science* 271:5255 (1996) 1560.
- [20] L.A. Strom, T.B. Sweeting, D.A. Norris and J.R. Morris, *Material Research Society Symposium – Fall Meeting*, Pittsburgh (1994) pp. 321–326.
- [21] T.B. Sweeting, D.A. Norris and L.A. Strom, *Materials Research Society Symposium – Fall Meeting*, Pittsburgh (1994) pp. 309–314.